SCIENTIFIC REPORTS

OPEN

Electroencephalographic derived network differences in Lewy body dementia compared to Alzheimer's disease patients

Received: 10 July 2017
Accepted: 5 March 2018
Published online: 15 March 2018

Luis R. Peraza[1], Ruth Cromarty[1], Xenia Kobeleva[2], Michael J. Firbank[1], Alison Killen[1], Sara Graziadio[3], Alan J. Thomas[1], John T. O'Brien[1,4] & John-Paul Taylor[1]

Dementia with Lewy bodies (DLB) and Alzheimer's disease (AD) require differential management despite presenting with symptomatic overlap. Currently, there is a need of inexpensive DLB biomarkers which can be fulfilled by electroencephalography (EEG). In this regard, an established electrophysiological difference in DLB is a decrease of dominant frequency (DF)—the frequency with the highest signal power between 4 and 15 Hz. Here, we investigated network connectivity in EEG signals acquired from DLB patients, and whether these networks were able to differentiate DLB from healthy controls (HCs) and associated dementias. We analysed EEG recordings from old adults: HCs, AD, DLB and Parkinson's disease dementia (PDD) patients. Brain networks were assessed with the minimum spanning tree (MST) within six EEG bands: delta, theta, high-theta, alpha, beta and DF. Patients showed lower alpha band connectivity and lower DF than HCs. DLB and PDD showed a randomised MST compared with HCs and AD in high-theta and alpha but not in DF. The MST randomisation in DLB and PDD reflects decreased brain efficiency as well as impaired neural synchronisation. However, the lack of network topology differences at the DF between all dementia groups and HCs may indicate a compensatory response of the brain to the neuropathology.

Dementia with Lewy bodies (DLB) and Alzheimer's disease (AD) are leading causes of neurodegenerative dementia in older adults. DLB is characterised by the core symptoms of visual hallucinations, cognitive fluctuation and Parkinsonism. Other symptoms may also be present and precede the core ones such as autonomic dysfunction, falls, and sleep disturbances[1]. In contrast, patients with AD compared to DLB often have more significant memory problems; including memory loss, difficulty recalling recent events and learning new information[2]. At early stages both dementias present with an important symptomatic overlap[3], e.g. problems with thinking and reasoning, leading to a frequent misdiagnosis of DLB patients as AD[4]. Another common cause of dementia linked to DLB is Parkinson's disease dementia (PDD); this condition shares symptomatic and pathologic overlaps with DLB[5]. However their clinical paths differ at the beginning of the disease; in DLB motor symptoms either occur concurrently with cognitive symptom onset or after, whereas PDD patients experience motor symptoms before the onset of cognitive decline[1]. AD and PDD offer two different disease perspectives for the understanding of DLB and this reflects the relative loading of pathology between the conditions, with DLB having both Alzheimer and alpha-synuclein pathology[6].

Electroencephalography (EEG) represents an important neuroimaging modality to study the effects of dementia in brain processes; previous work in the DLB field has been carried out by Bonanni, *et al.*[7], Stam, *et al.*[8] and Babiloni, *et al.*[9] amongst others[10–13], with the current consensus indicating that there is a slowing of the dominant frequency band (typically in the alpha frequency range) during eye-closed EEG at occipital regions in Lewy body dementia, and that this feature may be useful as a diagnostic biomarker of DLB versus AD[14]. The potential of this EEG feature as a DLB biomarker has been acknowledged as well by the recent consensus criteria for the clinical

[1]Institute of Neuroscience, Campus for Ageing and Vitality, Newcastle University, Newcastle upon Tyne, NE4 5PL, United Kingdom. [2]University Hospital Bonn, Clinic for Neurology, 53127, Bonn, Germany. [3]NIHR Newcastle In Vitro Diagnostics Co-operative, Newcastle-Upon-Tyne Hospitals NHS Foundation Trust, Newcastle upon Tyne, NE1 4LP, United Kingdom. [4]Department of Psychiatry, University of Cambridge School of Medicine, Cambridge, CB2 0SP, United Kingdom. Correspondence and requests for materials should be addressed to L.R.P. (email: luis.peraza-rodriguez@newcastle.ac.uk)

diagnosis of this dementia[15], where the slowing of the dominant band in patients has been given the status of supportive biomarker to differentiate DLB from AD[15]. Compared with other neuroimaging modalities, EEG has the advantage of being non-invasive, widely available and inexpensive. Additionally, EEG can be acquired multiple times without associated side effects[16].

The slowing of EEG frequencies in patients is commonly measured in quantitative EEG with the dominant frequency (DF). This DF is defined as the frequency with the highest power in the EEG spectrum[7] and expected to be located between 4 and 15 Hz. In this regard, Bonanni, *et al.*[17] showed a decrease of DF in DLB patients in occipital cortices compared with AD patients and healthy controls (HCs), and subtle differences when compared with PDD[17]. Additionally the authors also reported higher variability of DF in DLB patients which correlated with the level of cognitive fluctuations. Other proposed features which are gaining traction in dementia include that of brain networks[18], which offer an integrative perspective for the complex functional connectivity of the brain and of particular interest is the subnetwork known as the minimum spanning tree (MST)[19]. A brain network is represented within the framework of graph theory by a graph comprised of nodes and edges[20]; in EEG the nodes are the electrodes and the edges are the connectivity between electrodes. Network connectivity can be estimated with the phase lag index (PLI), a connectivity measure resistant to the effects of the scalp's volume conduction[21]. The MST is then the network which has the minimum number of strongest edges while connecting all nodes without cycling paths. Using this approach, Yu, *et al.*[22] reported that in AD there exists a decentralisation of the network tree towards a line-like less efficient configuration. In the DLB field, van Dellen, *et al.*[23] showed that patients present with a decreased EEG network efficiency, which the authors linked to impaired cognition.

In this investigation we studied brain network connectivity in EEG recordings from DLB, AD, PDD, and HC participants in the sensor domain using the MST, in order to find network differences in DLB compared with the other associated dementias and HCs. In light of previous investigations on band power differences in DLB, we investigated MST topology at different canonical frequency bands including the DF band. We hypothesised that network topology features and their variability consistently differ among our studied dementia groups, that these may have potential use as differential biomarkers in DLB diagnosis versus AD and that these features would correlate with clinical cognitive and memory scores. In addition, we hypothesised that the functional network topology of our patient groups in the DF band would highlight pathological mechanisms of dementia and neural degeneration.

Results

After EEG pre-processing, 6 AD, 1 HC, 1 DLB and 1 PDD participants were excluded from the final analysis because their cleaned EEG recordings had less than 50 seconds of continuous EEG, resulting in final groups of 17 HC, 26 AD, 25 DLB and 21 PDD participants.

Demographics. Demographics and clinical variables of our studied groups are given in Table 1. The recruited groups did not show significant differences in terms of age and gender. All patient groups were matched for global cognitive impairment by their CAMCOG and MMSE scores, although the AD group showed a trend of lower cognitive impairment compared with the other dementia groups. The memory domain in the CAMCOG was significantly lower in the AD group than in PDD and DLB. Complex visual hallucinations (NPI hall) and cognitive fluctuations (CAF) were, as expected, higher in both Lewy body dementias compared to AD patients. In relation to their medications, PDD patients were on higher doses of dopaminergic therapy than the DLB group, but there were not significant differences between the dementia groups in terms of use of cholinesterase inhibitor medications.

Dominant frequency and network measures. The one-way ANOVA tests were significant for differences in DF across the four participant groups; $F(85,3) = 6.75$, p-value $= 0.0004$. Post-hoc tests showed that DLBs had a significantly lower DF (DLB: mean $= 6.8$ Hz, SD $= 0.91$) than ADs (mean $= 7.5$ Hz, SD $= 1.21$) and HCs (mean $= 8.6$ Hz, SD $= 0.82$) but not when compared against the PDD group (PDD: mean $= 6.2$ Hz, SD $= 0.56$). The AD group showed a lower DF than HCs but it was higher than in the PDD group, Fig. 1. The one-way ANOVA for the dominant frequency variability (DFV) also showed significant differences; $F(85,3) = 4.59$, p-value $= 0.005$. The AD group presented with significantly higher variability (AD: mean $= 1.67$ Hz, SD $= 0.79$) compared with the other groups, and DLBs showed significantly lower DFV (DLB: mean $= 1.027$ Hz, SD $= 0.3$) when compared with AD, Fig. 1.

The two-way four-group ANOVA tests (group and frequency band effects) for the network structure measures within the six frequency bands, showed significant differences for the maximum nodal degree ($degree_{max}$), leaf ratio, eccentricity, network diameter and radius (see Methods for a full description of MST measures); these measures were significant for the group effect. The global effects for these measures showed a decreased $degree_{max}$ and leaf ratio in the three dementia groups compared with HCs, predominantly in the alpha band, while diameter, eccentricity and radius were higher in the dementia groups compared with HCs, predominantly in the high-theta band and with a trend for differences in the means of HC < AD < DLB < PDD, see Fig. 2 upper row. However, when analysing the post-hoc between-group differences in network topology for the DF band, none of the post-hoc tests were significant, with uncorrected p-values > 0.05, Fig. 2 bottom row.

The MST-PLI related measures (PLI mean, leaf, root and height) were significant for both mean and variability but mainly for the interaction effect of group and frequency band—see Fig. 3. Differences between groups were found predominantly in the theta, high-theta and alpha bands. Specifically, the HC group was significantly different when compared against the dementia groups for PLI measures in the alpha band. PLI height was significantly different between DLB and AD in the beta band.

Significant multiple linear regressions between the clinical variables and the network measures are shown in Table 2 and Fig. 4. None of the measures of variability related with the clinical variables, and we also tested these without the log-transformation with same results. For dominant frequency, the most significant relation

	HC (N = 17)		AD (N = 26)		DLB (N = 25)		PDD (N = 21)		p-value
Age	76.18	±5.65	76.46	±7.83	75.8	±6.5	73.29	±5.842	$F(3,85) = 1.03$, p-value = 0.380^{T}
Male/Female	10/7		18/8		20/5		19/2		$X^2(3, N = 89) = 5.89$, p-value = 0.117‡
MMSE	29.12	±0.857	20.08	±4.279	22.64	±4.3	22.71	±4.85	$F(2,69) = 2.81$; p-value = 0.067*
CAMCOG total	96.47	±3.69	66.54	±16.46	76.08	±12.92	73.38	±13.88	$F(2,69) = 2.89$; p-value = 0.063*
CAMCOG executive	22.71	±2.25	14.46	±5.49	13.12	±5.03	12.9	±2.86	$F(2,69) = 0.79$; p-value = 0.457*
CAMCOG memory	23.47	±2.035	10.88	±5.1	18.04	±4.9	17.48	±5.05	$F(2,69) = 15.5$; p-value < 0.001*
CAMCOG attention	6.76	±0.562	3.81	±2.514	4.4	±2.27	4.19	±1.721	$F(2,69) = 0.465$; p-value = 0.63*
NPI hall	0	0	0.04	±0.2	1.76	±1.86	2.57	±2.29	$F(2,68) = 14.1$; p-value < 0.001*
CAF total	0	0	0.6	±1.52	3.92	±4.142	6.63	±4.271	$t(42) = 2.12$, p-value = 0.03^{T}
Animal Categorical fluency	20.71	±5.71	11.15	±5.25	11.16	±3.88	11.33	±4.14	$F(2,69) = 0.011$; p-value = 0.989*
UPDRS III	1.24	±1.522	2.28	±1.929	15.52	±8.2	25.57	±7.018	$t(44) = 4.42$, p-value < 0.001^{T}
Angle discrimination	19.63	±0.88	18.24	±3.72	16.17	±4.85	16.55	±4.99	$H(2) = 4.1$, p-value = 0.129‡
FAS Verbal fluency	45.12	±16.53	25.96	±16.14	19.68	±12	20.81	±13.7	$H(2) = 1.94$, p-value = 0.378‡
LEDD	0	0	0	0	164.88	±231.6	818.23	±381.3	$t(44) = 7.15$, p-value < 0.001^{T}
AChEI (yes/no)	0/17		24/2		23/2		16/4†		$X^2(2, N = 71) = 2.13$, p-value = 0.346
Years since diagnosis	0	0	1.77	±1.13	0.87	±0.63	1.41	±1.91	$H(2) = 10.9$, p-value = 0.004‡

Table 1. Demographics and clinical variables. *ANOVA three groups (AD, DLB, PDD); ^{T}ANOVA four groups; $^{‡}\chi^2$ test four groups. ‡Unpaired t-test (DLB vs PDD); ‡Kruskal-Wallis three groups (AD, DLB, PDD). †One PDD patient was on Memantine.

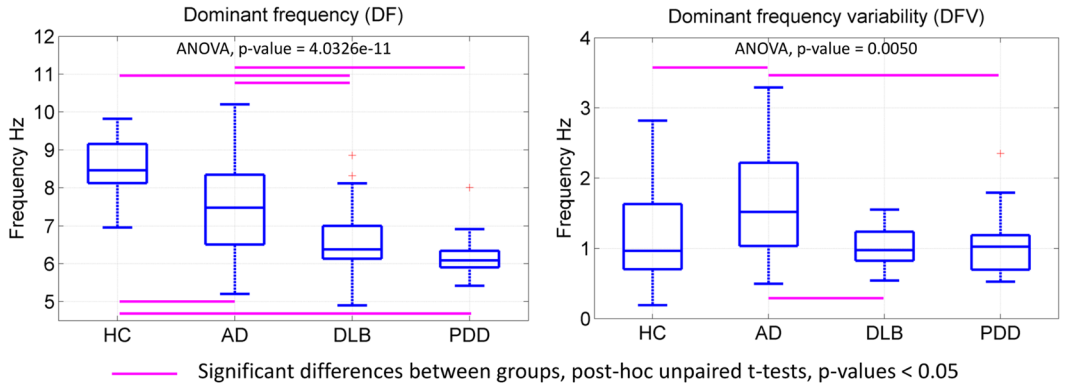

Figure 1. Dominant frequency (DF) and variability (DFV) box-plots. Four-group ANOVAs' p-values are given for each test, uncorrected. DF mean and standard deviation (SD) per group: HC (8.59 Hz, SD = 0.82), AD (7.5 Hz, SD = 1.21), DLB (6.8 Hz, SD = 0.91), PDD (6.2 Hz, SD = 0.56). DFV mean and SD per group: HC (1.21 Hz, SD = 0.67), AD (1.67 Hz, SD = 0.79), DLB (1.027 Hz, SD = 0.3), PDD (1.048 Hz, SD = 0.42). Each box in the plots shows the median as the central line, the extremes of each box are the first and third quartile and the whiskers represent the minimum and maximum values in the sample. DF and DFV were estimated from the occipital electrodes; see Supplementary Fig. S1.

was found between it and verbal fluency in all dementia groups with a positive correlation, and in AD and DLB for the within-group correlations, see Table 2. Dominant frequency was also significantly related to animal naming, CAMCOG, MMSE and Trail A test, and showed a positive relation between DF and cognitive impairment by these clinical measures. PLI tree measures in the theta band significantly related to cognitive variables. The network mean PLI in the high-theta band significantly related to the frequency and severity of complex visual hallucinations (NPI hall) in the DLB group, see Fig. 4. We also tested whether changing the reference group in the multiple linear regressions altered the results, which it did not. Additionally, we tested if Levodopa presented with a significant effect on the EEG features for the DLB and PDD groups. No effect was found between Levodopa medication and significant network measures. However, there was a significant group effect as result of the higher Levodopa doses in the PDD group (Supplementary Table S7).

Diagnostic analysis. MST measures that showed significant differences for the diagnostic scenarios including DF and DFV, were used in the classification analysis; the receiver operating characteristic curves for this analysis are shown in Fig. 5. AD vs DLB classification reached an 80% sensitivity (0.41–0.82 95% confidence internal CI), 85% specificity (0.42–0.92 CI) with 0.86 area under the curve (AUC). When differentiating DLB versus PDD,

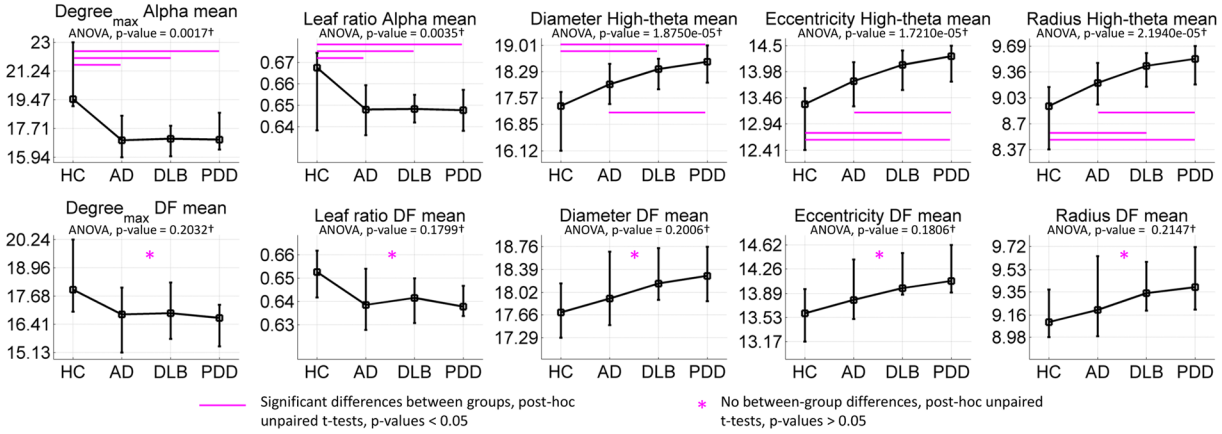

Figure 2. Two-way four-group ANOVA tests for the group effect. Upper row: The most significant post-hoc one-way ANOVAs per network measure and frequency band are shown. Significant (at p-value < 0.05 for the multiple unpaired t-tests) post-hoc between-group differences for the group means are indicated with line markers in magenta colour. Bottom row: post-hoc one-way ANOVA tests for the dominant frequency (DF) per network measure were nonsignificant. *Post-hoc multiple unpaired t-tests for comparisons between participant groups were also nonsignificant for the DF band. †ANOVA p-values are shown uncorrected for multiple comparisons; multiply by 72 for Bonferroni adjustment. For each plot, the line crosses the group means and the error bars span the first and third quartiles. Group effects are given in Supplementary Table S1 and their mean in Supplementary Table S2.

sensitivity was 76% (0.27–0.83 CI) and specificity was also 76% (0.58–0.88 CI); 0.77 AUC. Classification between HC and AD + DLB reached 0.96% sensitivity (0.78–1.0 CI) and 77% specificity (0.58–0.90 CI), 0.93 AUC. The step-wise multiple linear regression showed that for the AD vs DLB separation, the DFV was the best discriminant between both dementias (p-value = 0.0083) followed by PLI height in the beta band (p-value = 0.027). When diagnosing both combined groups AD + DLB versus the HC group, the step wise linear regression showed that the best discriminants were the PLI leaf mean in the alpha band (p-value < 0.0001) followed by DF (p-value < 0.0039). For the classification between DLB and PDD the PLI mean in the alpha band was the best discriminant between both groups (p-value = 0.0012).

Discussion

Our analysis showed significant differences between the dementia groups and HCs for DF and PLI network measures. We confirmed the well-established finding that there is a slowing of DF in the Lewy body dementias—DLB and PDD—compared with AD and HCs in the occipital regions[9,16,24,25]. Additionally, we explored the variability of DF between the studied groups and we demonstrated that DFV is higher in AD compared with HCs and both Lewy body dementia groups. Differences between the MST measures were significant at several frequency bands; theta, high-theta and alpha. However, PLI height scores in the beta band were shown to be lower in DLB compared with AD patients.

PLI height is a measure of focused synchronisation in the root node (high PLI values and $degree_{max}$) and to be higher requires the existence of leaves far away from the root with low PLI connections, these latter lower than the root node connections[26]. A decrease in PLI height will therefore occur in two scenarios: (1) a star-like topology where the majority of edges connecting the root and leaf nodes are the same or (2) a PLI random connectivity matrix, where there are not significant differences in PLI strength between leaf edges and root edges. Our results suggests the latter case, i.e. that our DLB and PDD groups present with a randomisation of the MST. This is observed by the global effects of the network measures; the lower $degree_{max}$ and leaf ratio in the alpha band combined with higher network diameter, eccentricity and radius in the high-theta band indicate network randomisation, and a decrease in global efficiency of the MST. Similar results were reported by Olde Dubbelink, *et al.*[27] and Utianski, *et al.*[28] who showed than in PD and PDD respectively, there exists a less "star-like" network topology or as Yu, *et al.*[22] reported, a "line-like" topology in dementia patients. Specifically, Utianski, *et al.*[28] reported decreased number of MST leaves in PD patients. A more line-like network topology suggests a desynchronization of neural communication, where the brain network of dementia patients fails to engage in focused regional synchronisations which may happen at different locations depending on the brain's dynamics. Visualisation of these MST network characteristics in four representative participants is shown in Fig. 6, for the alpha and DF bands. The star-like topology can be easily observed in the HC participant where two highly connected nodes comprise the centre of the star. The randomised tree or line-like topology can be observed easier in the DLB patient in the dominant frequency example (bottom row); nodes here are not highly connected (low $degree_{max}$) and several nodes are connected within the same path in a sequence, i.e. lines.

In a previous investigation, van Dellen, *et al.*[23] reported a PLI decrease in the alpha band of DLB patients compared to AD and HCs. This contrasts somewhat with our investigation where PLI alpha was not significantly different between AD and DLB, although we demonstrated that it was lower in both dementias when compared with HCs. Instead we found that there are PLI differences in the high-theta and beta band between AD and DLB. PLI

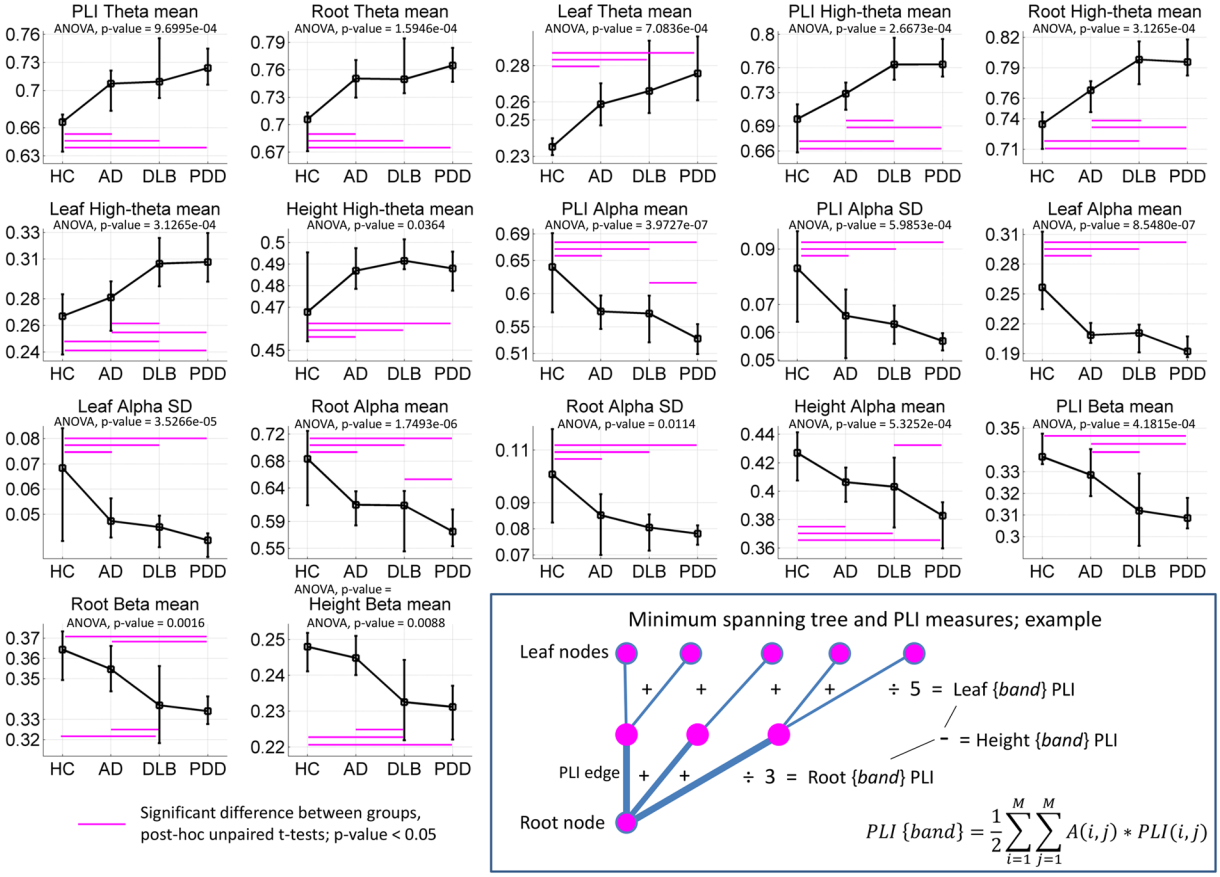

Figure 3. Minimum spanning tree measures that showed significant differences across the groups of interests; ANOVA tests' p-values are shown Bonferroni adjusted, i.e. multiplied by a correction factor that accounts for the 72 post-hoc one-way ANOVA tests. Significant multiple unpaired t-tests, p-value < 0.05, within each one-way ANOVA test are shown with line markers (in magenta colour) for the two groups with different means. For each plot, the line crosses the group means and the error bars span the first and third quartiles; mean and standard deviation are given in Supplementary Table S4. Bottom-right: Minimum spanning tree example comprising nine nodes and eight edges, where five of them connect leaf nodes. *A(i, j)* is the network adjacency matrix where an edge between nodes *i* and *j* is indicated with 1, and 0 otherwise. *PLI(i, j)* is the PLI score between nodes *i* and *j*. *M* is the total number of electrode nodes. See Supplementary Table S3 for variable meaning.

alpha band differences in our study occurred when comparing HCs against all dementia groups but not between the dementia groups. This suggests that PLI in the alpha band is a marker of healthy brain but that it is not specific enough to differentiate between dementias[9].

Exploratory diagnostic classification between AD and DLB was achieved by MST-PLI measures in the high-theta and beta bands as well as DF and DFV with high sensitivity and specificity of 80% and 85% respectively, and which is comparable to FP-CIT SPECT imaging[29]. For this classification analysis, the most significant discriminant was the larger DFV in the AD group followed by the lower PLI height in beta band in the DLB group. This contrasts with the results by Bonanni, *et al.*[17] who reported higher DFV in DLB patients compared to AD ones and higher DFV than HCs for both dementia groups[17]. This result disagreement may be driven by cohort specific differences or by the estimating method for DFV; here DFV was defined as the standard deviation of the DF throughout the EEG segments, while in Bonanni, *et al.*[17] DFV was defined using a visual rating of DF range on sequential EEG segments. Previous investigations using EEG features have reported similar or higher classification rates when differentiating Lewy body dementias and AD groups. For instance, Garn, *et al.*[30] reported 100% accuracy separating AD from a group of DLB-PDD patients using 25 EEG features, and Snaedal, *et al.*[31] reported an accuracy of 91% in a similar group set-up using 37 EEG features. It is difficult to compare the performance between these investigations and ours due to differences in adopted approaches (the latter focussed on canonical spatial-temporal EEG features compared to our work which additionally used graph theory derived metrics/features) and number of features used for classification (nine features in our investigation). Additionally, these two previous reports[30,31] used a collated DLB-PDD group which may have biased the group classification as PDD patients may be closer to PD in the Lewy body spectrum[5,32] and neuropathologically further away from AD in contrast to DLB. In this investigation, we decided to keep our PDD and DLB groups separated since there is a clinical interest on the correct diagnosis of DLB versus AD, but not so much between AD and PDD given PDD

Network variable	Clinical variable	Linear regression [AD + DLB + PDD]		HC	AD	DLB	PDD
		B_1	B_1 p-value	ρ (p-value)	ρ (p-value)	ρ (p-value)	ρ (p-value)
PLI high-theta mean	NPI hallucinations	−9.87	0.0463	— (–)	0.047 (0.824)	−0.498 (0.011)	−0.127 (0.584)
PLI theta mean	Animal naming	−31.47	0.0400	0.22 (0.398)	−0.36 (0.075)	−0.31 (0.129)	0.05 (0.842)
PLI theta mean	CAMCOG memory	−39.83	0.0204	−0.04 (0.866)	−0.23 (0.261)	−0.31 (0.137)	−0.33 (0.147)
PLI theta mean	CAMCOG total	−119.70	0.0153	0.06 (0.834)	−0.33 (0.105)	−0.32 (0.116)	−0.21 (0.361)
Leaf theta mean	Animal naming	−48.14	0.0221	0.02 (0.938)	−0.43 (0.027)	−0.32 (0.120)	−0.02 (0.933)
Leaf theta mean	CAMCOG memory	−58.91	0.0125	0.19 (0.460)	−0.31 (0.130)	−0.28 (0.174)	−0.36 (0.113)
Leaf theta mean	CAMCOG total	−169.77	0.0124	0.21 (0.430)	−0.37 (0.061)	−0.33 (0.110)	−0.21 (0.373)
Root theta mean	CAMCOG memory	−43.24	0.0196	−0.03 (0.914)	−0.17 (0.395)	−0.29 (0.148)	−0.43 (0.054)
Root theta mean	CAMCOG total	−126.38	0.0178	0.07 (0.788)	−0.25 (0.220)	−0.32 (0.124)	−0.32 (0.161)
Dominant frequency	Animal naming	1.36	0.0131	0.3 (0.244)	0.41 (0.040)	0.25 (0.230)	0.03 (0.902)
Dominant frequency	CAMCOG attention	0.59	0.0317	−0.27 (0.292)	0.34 (0.088)	0.38 (0.062)	−0.38 (0.091)
Dominant frequency	CAMCOG executive	1.54	0.0071	0.22 (0.393)	0.38 (0.056)	0.32 (0.124)	0.02 (0.918)
Dominant frequency	CAMCOG total	5.24	0.0029	0.08 (0.756)	0.5 (0.010)	0.33 (0.104)	−0.05 (0.819)
Dominant frequency	MMSE	1.19	0.0294	−0.25 (0.336)	0.45 (0.021)	0.30 (0.141)	−0.2 (0.389)
Dominant frequency	Trail A	−21.88	0.0266	−0.28 (0.270)	−0.42 (0.034)	−0.27 (0.220)	−0.39 (0.112)
Dominant frequency	Verbal fluency	6.93	3.69E-05	0.20 (0.439)	0.59 (0.002)	0.52 (0.008)	0.16 (0.559)

Table 2. Multiple linear regressions controlling for group membership with two dichotomous variables (D) for the Lewy body dementia groups. Model: Clinical variable ~ β_1*network variable + β_2*D_{DLB} + β_2*D_{PDD}. Shown p-values correspond to the β_1 coefficient for the network variable in the regression model and are shown uncorrected. Within group Pearson's correlation and p-values are also given; full model's coefficients are given in Supplementary Table S5.

patients are diagnosed with PD prior to the onset of dementia[33]. Related to this, a recent report by Babiloni, *et al.*[9] showed a 69.7% accuracy differentiating AD from DLB (64.7% sensitivity, 73.8% specificity) using only three EEG features associated with occipital alpha and delta power. However, higher diagnostic classification can be achieved by combining neuroimaging modalities. For instance, Colloby, *et al.*[13] reported 86% sensitivity and 93% specificity (90% accuracy) classification for DLB versus AD, using a combined EEG-structural MRI approach. Forward projection of the MST-PLI and DF measures presented here, onto independent EEG samples will be required to clarify the robustness of these measures as diagnostic tools for DLB.

DF and MST-PLI frequency scores significantly related with cognitive variables in our patients, suggesting a pathological relation with dementia. The verbal fluency test, which measures executive function, was highly positively correlated with DF in the dementia groups. Complex visual hallucinations (severity and frequency) was related with PLI mean in high-theta band, and significantly correlated within the DLB group, see Table 2. To date, we are not aware of previous investigations reporting a relation between complex visual hallucinations and resting state EEG features in DLB; this core symptom is frequently studied with event related responses[34,35] or transcranial stimulations[36]. However, previous EEG investigations in the Charles Bonnet syndrome (CBS) which is characterised by complex visual hallucinations in people with partial or severe blindness, have reported alterations in alpha and theta power[37,38] and this agrees with our results. Nevertheless, we must also take into account that our multiple linear regression results are uncorrected, and thus these findings must be taken with caution.

None of the MST measures were significantly different between groups for the individualised DF band in measures related to network structure such as diameter, radius and eccentricity; see Fig. 2 bottom row. This suggests that in dementia, the EEG network which is present at lower dominant frequencies and whilst these dominant frequencies are pathological, it is still a network which would have been present in the premorbid state with normal structural neural communications, and thus may represent a reactive or compensation state[39]. A recent EEG investigation on brain connectivity by Frantzidis *et al.*[39] reported compensation in participants with mild cognitive impairment (MCI), a condition that often preludes the onset of AD. They demonstrated the presence of densely connected regions in the networks of MCI participants but not in healthy controls, which the authors attributed to a compensation mechanism at early disease stages. Brain compensation is a phenomenon reported as well in functional magnetic resonance imaging (fMRI) research[40]. In fMRI, compensation is expressed and interpreted as an over-recruitment of neural circuits in order to maintain cognitive levels or motor processes in the presence of disease. In this regard, computational models of cortical activity have proven that the resonance frequency—dominant frequency—of neural circuits is inversely proportional to the size of the excited tissue[41], i.e. larger networks communicate at lower frequencies[42]. These investigations thus suggest that the decrease of dominant frequency observed in our Lewy body dementia and Alzheimer's disease participants may be an effect of over-recruitment of neural tissue in order to maintain a dynamic network structure similar to healthy controls; or in other words, recruitment of larger neural circuits needed for compensation is implemented by the brain at lower frequencies. It is suggested that the slowing of DF is driven by neurodegeneration of the cholinergic system not only in parkinsonian diseases[43] but also in AD[44]. Evidence for this comes from EEG investigations analysing the effect of cholinesterase inhibitors and the partial restoration of alpha band power after medication[45,46]. Our results then propose a complementary perspective of these previous findings for the relation between cholinergic dysfunction in dementia and DF slowing as a compensatory mechanism.

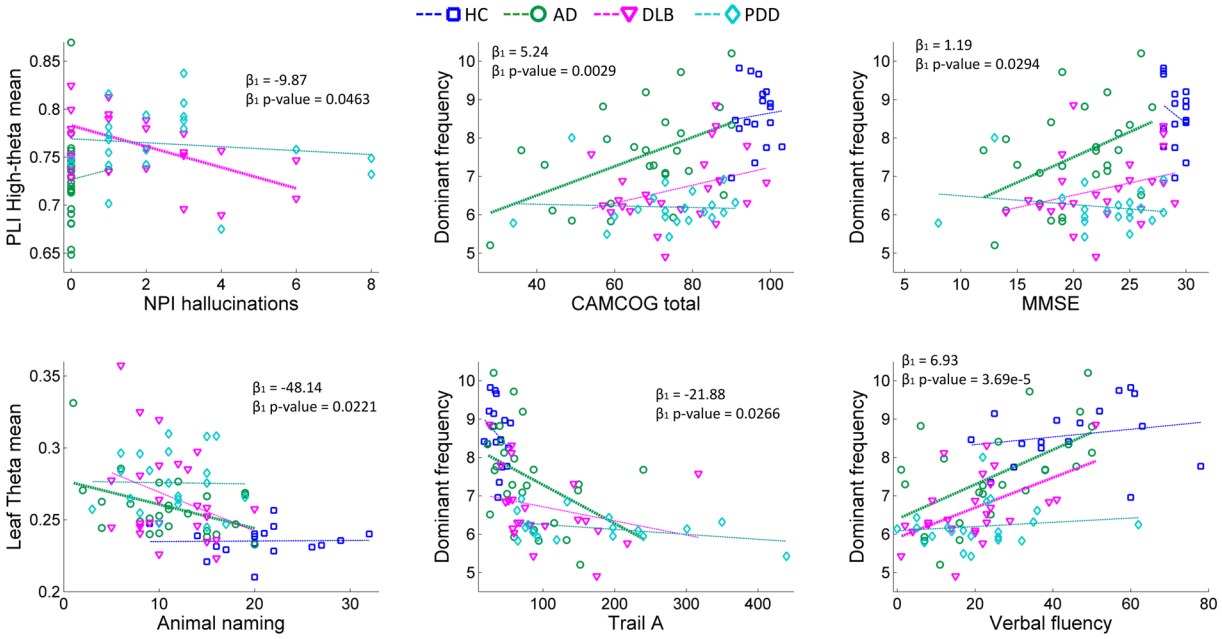

Figure 4. Selected significant multiple liner regressions between clinical variables and network measures. *P-values for the β_1 coefficient for network measure are shown uncorrected. Significant within group Pearson's correlations, at p-value < 0.05, are shown with thicker dashed lines; see Table 2 for all significant results. Model: Clinical variable $\sim\beta_1$*network variable $+\beta_2$*$D_{DLB} + \beta_2$*D_{PDD} + Intercept, where D is a dichotomous vector for each of the Lewy body dementia groups.

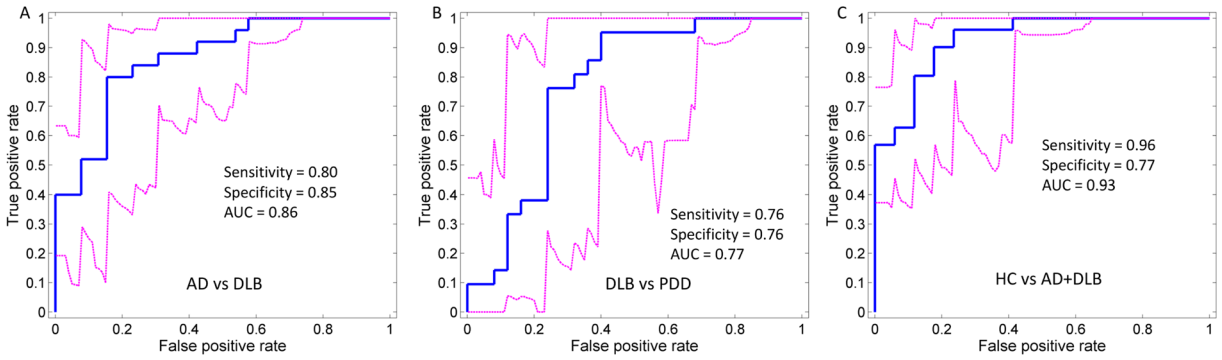

Figure 5. Receiver operating characteristic (ROC) curves by logistic regression for each of the diagnostic scenarios analysed, see Supplementary Table S6. Magenta dashed lines show the 95% confidence intervals for the ROC curves; bootstrapping with 5000 iterations implemented with the perfcurve MATLAB function. Optimal sensitivity and specificity as well as the area under the curve (AUC) are shown within each curve plot.

Our investigation has some limitations. First, all patients were medicated at the time of assessment and potentially on agents which are known to alter EEG and could, for example, partially restore alpha power in patients. Despite this, we were able to find robust differences between patients and healthy controls and our results were in agreement with previous work in the field. Also, eyes-open EEG was not investigated in the current report which may offer higher diagnostic ratios if combined with features from eye-closed EEG. We were also unable to test our studied network features for disease progression, since we do not have longitudinal patient data. Ideally, EEG biomarkers for DLB should be investigated in the prodromal phase of the disease when clinical diagnosis is uncertain[47], and with follow-up patient assessments; certainly early and distinct EEG changes are evident in MCI patients who go on to develop dementia[7]. Finally, the MST approach followed in the current investigation does not provide regional measures of network connectivity which may offer as well other important features for diagnostic classification and disease progression[27]. Future research will be needed to investigate all these possibilities including external validation of biomarkers. This work represents a first step in biomarker discovery and further investigations to evaluate cost-effectiveness, increased patient benefits in comparison with the current diagnostic standard, and feasibility of introduction of such biomarkers in the current care pathway are needed before these indexes can be proposed as validated biomarkers.

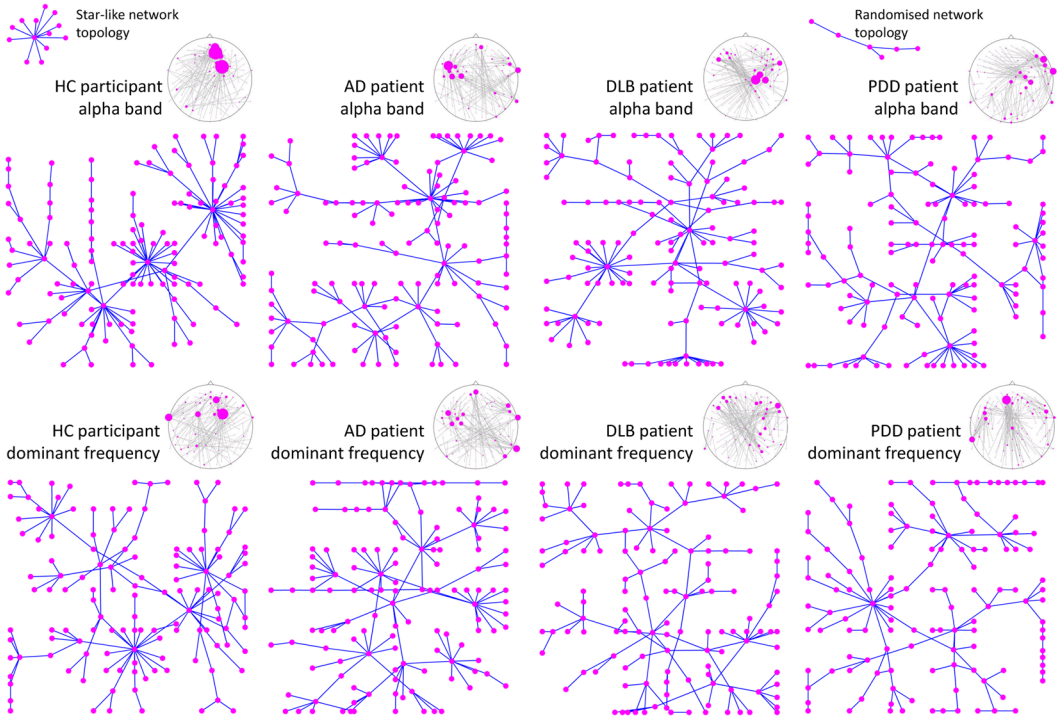

Figure 6. EEG minimum spanning tree examples from representative participants. Each participant was chosen as representative for being the median of their respective groups according to the leaf ratio mean in the alpha band. Similarly, the dominant frequency tree is also shown for the same participants. Notice the distinguishable "star-like" topology for the alpha-band network tree of the healthy control (HC) with two nodes with high nodal degree, and the more random tree in Lewy body dementia patients with a "line-like" topology; dementia with Lewy bodies (DLB) and Parkinson's disease dementia (PDD). The Alzheimer's disease (AD) patient also shows a star-like topology, although not as evident as the HC, suggesting impaired network. At the top of each network tree, the same network is shown on an EEG 10-5 system layout; here the diameter of the EEG electrodes is proportional to their nodal degree.

In conclusion, we found that the alpha band and its related MST network measures are markers of healthy brain as compared with dementia, while DLB and AD patients differentiated in DFV and PLI height in the beta band, and that these measures resulted of higher utility as potential diagnostic biomarkers. We demonstrated that DLB as well as PDD present with a randomised or line-like MST network compared to HCs, and this suggests a decrease in focused neuronal synchronisation in these patients for the high-theta and alpha bands. In contrast, we found potential evidence of compensation in the functional network within the dominant frequency band, where no differences were found between our dementia groups and healthy controls for the topology of their MSTs.

Methods

Participants and clinical assessments. A total of 98 old adult participants were recruited within the North East of England. Dementia patients were recruited from a population referred to old age psychiatry and neurology services: 32 patients with AD (22 male, 10 female), 26 patients with DLB (21 male, 5 female), and 22 patients diagnosed with PDD (20 male, 2 female). Additionally, 18 healthy controls (HC) were recruited for group comparisons (11 male, 7 female). Patient groups were diagnosed by two experienced clinicians according to the clinical diagnosis criteria for these dementias: The dementia with Lewy bodies consensus criteria[1,15], the diagnostic criteria for PDD[33], and the National Institute on Aging-Alzheimer's Association criteria for AD[48].

All participants underwent comprehensive neurological and neuropsychiatric examinations. Specific tests relevant to the present study included the Mini-mental state examination (MMSE), the Cambridge cognitive battery tests (CAMCOG) as measures of global cognition as well as trail making test A, animal naming, FAS verbal fluency and visual perception (angle discrimination task). The latter tests, representative of executive and visuo-perceptual function, are often disproportionately affected in LBD and thus considered as key additional cognitive measures for correlation against our MST metrics. To assess whether MST alterations were associated with other core symptoms of LBD such as motor parkinsonism, cognitive fluctuations and visual hallucinations, the Unified Parkinson's Disease rating scale part III (UPDRS III), cognitive assessment of fluctuations (CAF)[49] scale, and the neuropsychiatric inventory test subscale for the severity and frequency of hallucinations (NPI hallucinations) were assessed; for the latter, carers were specifically asked about visual hallucinations rather than hallucinations in other modalities[50]. For patients that were on dopaminergic therapy, the Levodopa equivalent daily dose (LEDD) was estimated[51]. A MMSE score <8 for patients and <26 for the HC group was used as exclusion criteria. None of the recruited healthy participants had a history of neurological or psychiatric conditions and neither did the patients outside their core dementia.

Patients with Parkinsonism and on dopaminergic therapy were studied in the "ON" state. Ethical approval for this study was given by the Northumberland Tyne and Wear NHS Trust and Newcastle University ethics committee, and all methods in this study followed approved research guidelines by the mentioned ethics committee. All participants gave written informed consent prior study participation.

Electroencephalography and signal processing. Resting EEG recordings were acquired with Waveguard caps (ANT Neuro, The Netherlands) comprising 128 sintered Ag/AgCl electrodes placed in a 10–5 positioning system[52]. Channels were recorded with a sampling frequency of 1024 Hz and electrode impedance of <5 KΩ. At recording, all electrodes were referenced to Fz channel and the ground electrode was attached to the right clavicle. 150 seconds of continuous EEG resting state eyes closed were stored for off-line data processing, participants were seated throughout the recording and instructed to remain awake and as still as possible.

All pre-processing steps were carried out blinded to group membership and implemented with EEGLAB[53] MATLAB functions (R2012; MathWorks, Natick Massachusetts). 1) EEG channels had their baseline component subtracted and were band pass filtered between 0.3 Hz and 54 Hz with a second order Butterworth filter. 2) Bad channels were deleted including the reference electrode Fz; mean of four channels, with minimum one and maximums of 10 channels deleted. 3) Independent component analysis (ICA) with the FastICA[54] algorithm using default parameters was run for the entire EEG recording and up to 12 artefactual independent components were deleted. At this step special interest was put on identifying eye blink, cardiac and the 50 Hz power line components, i.e. components that were noisy throughout the EEG recording. 4) If after component deletion artefactual components were still identified, FastICA algorithm was run again and up to 6 artefactual components were deleted. 5) Noisy EEG segments with artefacts affecting all channels (e.g. muscle artefacts) were deleted. 6) EEG components were remixed to the sensor domain. 7) Previously deleted bad channels were spatially interpolated with EEGLAB using spherical interpolation. 8) As final step, the electrode montage was modified to average montage[55]. Participants with less than 50 seconds of continuous EEG after artefact cleaning were excluded from the remaining of the analysis. Curated and raw 50-second EEGs signals as well as anonymised clinical data are available upon request from the senior author (J-PT).

Dominant Frequency and its variability. Dominant frequency (DF) was estimated for the 50 second EEG segments. First, occipital channels (PO and O channels) were averaged to obtain a representative signal from this region, see Supplementary Fig. S1. Power spectral density was then estimated with Welch's periodogram; 2048 sample segments tapered with a Hamming window, 50% overlap between segments and a fast Fourier transform size of 2^13; these parameters led to a frequency resolution of 0.125 Hz. We defined DF as the frequency bin in the power spectrum with highest power between 4 and 15 Hz. DF for each participant was then estimated as the mean dominant frequency across the 49 windowed segments and DF variability (DFV) was defined as the standard deviation (SD) across the segments.

Phase lag index. Phase lag index (PLI) was chosen to measure the regional relation among all electrode pairs[56]. Briefly, PLI uses the Hilbert transform to estimate consistent causal delay between two signal sources and it has been proven that this measure is less affected by the scalp's volume conduction, a problem with other measures such as spectral coherence or Pearson's correlation[55]. PLI scores are bounded between 0 and 1, where 0 means lack of causal synchronisation and 1 full causal synchronisation. In this investigation, PLI was estimated for six frequency bands: the standard EEG delta (0.5–4 Hz), theta (4–5.5 Hz), high-theta (5.5–8 Hz), alpha (8–13 Hz), beta (13–30 Hz) and the dominant frequency band (DF $\pm$ 2 Hz) whose centre was participant specific. Frequencies >30 Hz were not studied since these are particularly affected by muscle artifacts, eye movement and microsaccades[57,58]. To compute the PLI scores, the 50 second EEG recordings were first filtered at each of the defined frequency bands using a second order Butterworth band-pass filter, then Hilbert-transformed and finally segmented into two-second segments with one second overlap leading to a total of 49 segments. After this, 49 PLI connectivity matrices of dimension 128×128 elements were computed for each two-second segment, frequency band and participant.

Minimum spanning tree. The minimum spanning tree (MST) in EEG networks is a subgraph which encompasses the strongest edges within the connectivity matrices, and reaches all nodes without creating cycling paths[19]. Here the edges of the network are represented by their connectivity strength given by the PLI scores and the nodes of the network are the electrodes. The Prim's algorithm[59] was used to estimate the MST with one minus the PLI score as input. Then, 10 MST measures and their variability (mean and SD; thus providing a total of 20 measures) were estimated for each frequency and participant. These measures are:

Maximum betweenness centrality (BC_{max}). Is a measure of hubness or centrality[60] and it is proportional to the number of shortest paths that crosses a node in the tree[61]. A node with high BC indicates high reachability of that node throughout the network. BC_{max} then represents the node with highest BC in the MST[62], and decreased BC_{max} suggests that the MST has decreased global efficiency[19].

Diameter. This is the largest distance or number of edges between any two nodes in the tree. An increased diameter indicates decreased network efficiency[28].

Eccentricity. Is the maximum distance or number of edges between a node and any other node in the tree. Here we summarised this measure as the average eccentricity across all nodes in the tree[62]. Increased eccentricity in the MST suggests decreased network efficiency.

Radius. The smallest node eccentricity in the tree.

Maximum degree (degree$_{max}$). The degree of a node equals the number of edges connected to that node. The degree$_{max}$ is the highest degree in the MST and belongs to the most connected node in the network[62]. This is a measure of focused synchronisation, and the highest possible degree$_{max}$ score would correspond to a MST that has a "star" topology[19] with only one central node connected.

Leaf ratio. The number of nodes connected to the MST by only one edge divided by the maximum number of possible leaves (M-1), where M equals 128 electrode nodes in this investigation.

PLI mean. The mean PLI score across the entire MST network.

PLI leaf. The mean PLI for all the edges connected to the leaf nodes.

PLI root. The mean PLI for the root node of the MST. Here the root is defined as node with the highest degree. Hence, PLI root is the mean PLI score for the edges connected to the node with highest degree in the MST.

PLI height. The difference between PLI root minus PLI leaf. PLI root equals the PLI leaf score if the MST has a star configuration[19].

MST measures were computed using functions from the Brain Connectivity[63] and the Network Analysis[64] toolboxes, as well as in-house functions in MATLAB.

Statistics. Statistical tests for the clinical and demographic variables were implemented in SPSS (Statistical Package for the Social Sciences v22, IBM) and these are defined in Table 1. All EEG scores of variability, standard deviations and DFV, were log-transformed to approximate their distribution to a Gaussian. Differences in DF and DFV were investigated with a one-way ANOVA for the four groups and post-hoc unpaired t-tests for between group comparisons. Significance of MST measures was assessed in three steps. First, significant differences were investigated with two-way four-group ANOVAs for each MST measure as dependant variable and the following factors as independent variables: group (HC, AD, DLB, and PDD), frequency (delta, theta, high-theta, alpha, beta, and DF) and their interaction (group and frequency). Null hypotheses were rejected if either the diagnosis or the interaction effects were significant at a p-value < 0.0025 thus accounting for the 20 MST measures assessed, i.e. Bonferroni correction. Secondly, for the significant two-way ANOVAs, post-hoc multiple one-way ANOVAs at each frequency band were evaluated and their significance was again Bonferroni corrected by the number of post-hoc tests, leading to an uncorrected p-value threshold of <0.0007 (since 12 two-way ANOVAs survived the first stage of tests). Finally, group differences were assessed with multiple unpaired t-tests. For this latter step we were interested in three exploratory diagnostic scenarios of significant difference: AD vs DLB, DLB vs PDD and HC vs both AD and DLB (AD + DLB). Notice that differences in DF is a hypothesized test based on previous literature and as such the post-hoc tests of the one-way ANOVA are uncorrected, while the two-way four-group ANOVA tests for the multiple network measures are corrected for multiple tests or comparisons.

In order to assess relations of network measures with the clinical variables in our dementia patients, we implemented a multiple linear regression for the three dementia groups with clinical variable as the dependant variable and the network measure as the independent variable. Additionally, we included two dichotomous regressors for the DLB and PDD groups, in order to account for the group effects. The AD group was left as the reference group for being the largest group in our investigation. Before regression analysis, all measures of variability including DFV were log-transformed to approximate their distribution to Gaussian. The regression was considered significant if the first coefficient of the model (β_1 for the network measure) was significant at a p-value < 0.05. The effect of Levodopa medication (LEDD) was assessed with multiple regression for the DLB and PDD groups, with one dichotomous variable to account for the group effect.

To assess the diagnostic accuracy of the studied measures in the three diagnostic scenarios, we implemented a logistic regression classification (Matlab functions glmfit.m and glmval.m); sensitivity, specificity and area under the curve (AUC) were computed for each scenario; confidence intervals were estimated by statistical bootstrapping with 5000 iterations (Matlab function perfcurve.m). For the DLB vs AD case, scores from the PLI mean, PLI leaf mean, PLI root mean in the high-theta band, PLI mean, PLI root mean, PLI height mean in the beta band, DF and DFV were used as regressors. For DLB vs PDD, scores from the PLI mean, PLI root mean and PLI height mean in the alpha band were used in the logistic regression. The HC vs AD + DLB diagnostic scenario used twelve network features as regressors which also showed significant differences, Supplementary Table S6. Diagnostic classification of HC vs PDD was not implemented. In order to find the most significant discriminants for the three diagnostic scenarios a stepwise multiple linear regression was implemented.

Network display and layout. In order to observe network topology characteristics within our studied groups, participants at the group median for the leaf ratio mean in the alpha band were selected as representative of each group. Leaf ratio mean scores were chosen for being consistently higher in the HCs compared with the dementia groups but not between the dementias. For each selected participant, the 49 PLI connectivity matrices were averaged. From the mean connectivity matrix, the MST was extracted and displayed using a forced-directed graph layout[64], which facilitates graph visualisation by minimising edge crossings. This procedure was also repeated for the DF band for the same participants.

References

1. McKeith, I. G. *et al*. Diagnosis and management of dementia with Lewy bodies: third report of the DLB Consortium. *Neurology* **65**, 1863–1872, https://doi.org/10.1212/01.wnl.0000187889.17253.b1 (2005).
2. Hanyu, H. *et al*. Differences in clinical course between dementia with Lewy bodies and Alzheimer's disease. *European journal of neurology: the official journal of the European Federation of Neurological Societies* **16**, 212–217, https://doi.org/10.1111/j.1468-1331.2008.02388.x (2009).
3. Tiraboschi, P. *et al*. What best differentiates Lewy body from Alzheimer's disease in early-stage dementia? *Brain: a journal of neurology* **129**, 729–735, https://doi.org/10.1093/brain/awh725 (2006).
4. Merdes, A. R. *et al*. Influence of Alzheimer pathology on clinical diagnostic accuracy in dementia with Lewy bodies. *Neurology* **60**, 1586–1590 (2003).
5. McKeith, I. Dementia with Lewy bodies and Parkinson's disease with dementia: where two worlds collide. *Practical neurology* **7**, 374–382, https://doi.org/10.1136/jnnp.2007.134163 (2007).
6. Metzler-Baddeley, C. A Review of Cognitive Impairments in Dementia with Lewy Bodies Relative to Alzheimer's Disease and Parkinson's Disease with Dementia. *Cortex* **43**, 583–600, https://doi.org/10.1016/S0010-9452(08)70489-1 (2007).
7. Bonanni, L. *et al*. Quantitative electroencephalogram utility in predicting conversion of mild cognitive impairment to dementia with Lewy bodies. *Neurobiology of aging*, https://doi.org/10.1016/j.neurobiolaging.2014.07.009 (2014).
8. Stam, C. J. *et al*. Graph theoretical analysis of magnetoencephalographic functional connectivity in Alzheimer's disease. *Brain: a journal of neurology* **132**, 213–224, https://doi.org/10.1093/brain/awn262 (2009).
9. Babiloni, C. *et al*. Abnormalities of cortical neural synchronization mechanisms in patients with dementia due to Alzheimer's and Lewy body diseases: an EEG study. *Neurobiology of aging* **55**, 143–158, https://doi.org/10.1016/j.neurobiolaging.2017.03.030 (2017).
10. Kai, T., Asai, Y., Sakuma, K., Koeda, T. & Nakashima, K. Quantitative electroencephalogram analysis in dementia with Lewy bodies and Alzheimer's disease. *Journal of the neurological sciences* **237**, 89–95, https://doi.org/10.1016/j.jns.2005.05.017 (2005).
11. Andersson, M., Hansson, O., Minthon, L., Rosen, I. & Londos, E. Electroencephalogram variability in dementia with lewy bodies, Alzheimer's disease and controls. *Dementia and geriatric cognitive disorders* **26**, 284–290, https://doi.org/10.1159/000160962 (2008).
12. Walker, M. P. *et al*. Quantifying fluctuation in dementia with Lewy bodies, Alzheimer's disease, and vascular dementia. *Neurology* **54**, 1616–1625 (2000).
13. Colloby, S. J. *et al*. Multimodal EEG-MRI in the differential diagnosis of Alzheimer's disease and dementia with Lewy bodies. *Journal of psychiatric research* **78**, 48–55, https://doi.org/10.1016/j.jpsychires.2016.03.010 (2016).
14. Olde Dubbelink, K. T. *et al*. Cognitive decline in Parkinson's disease is associated with slowing of resting-state brain activity: a longitudinal study. *Neurobiology of aging* **34**, 408–418, https://doi.org/10.1016/j.neurobiolaging.2012.02.029 (2013).
15. McKeith, I. G. *et al*. Diagnosis and management of dementia with Lewy bodies: Fourth consensus report of the DLB Consortium. *Neurology* **89**, 88–100, https://doi.org/10.1212/wnl.0000000000004058 (2017).
16. Cromarty, R. A. *et al*. Neurophysiological biomarkers for Lewy body dementias. *Clinical Neurophysiology*, https://doi.org/10.1016/j.clinph.2015.06.020 (2016).
17. Bonanni, L. *et al*. EEG comparisons in early Alzheimer's disease, dementia with Lewy bodies and Parkinson's disease with dementia patients with a 2-year follow-up. *Brain: a journal of neurology* **131**, 690–705, https://doi.org/10.1093/brain/awm322 (2008).
18. Sporns, O., Chialvo, D. R., Kaiser, M. & Hilgetag, C. C. Organization, development and function of complex brain networks. *Trends in cognitive sciences* **8**, 418–425, https://doi.org/10.1016/j.tics.2004.07.008 (2004).
19. Stam, C. J. *et al*. The trees and the forest: Characterization of complex brain networks with minimum spanning trees. *International journal of psychophysiology: official journal of the International Organization of Psychophysiology* **92**, 129–138, https://doi.org/10.1016/j.ijpsycho.2014.04.001 (2014).
20. Sporns, O. Structure and function of complex brain networks. *Dialogues in Clinical Neuroscience* **15**, 247–262 (2013).
21. Nunez, P. L. & Srinivasan, R. *Electric fields of the brain: the neurophysics of EEG*. (Oxford University Press, USA, 2006).
22. Yu, M. *et al*. Different functional connectivity and network topology in behavioral variant of frontotemporal dementia and Alzheimer's disease: an EEG study. *Neurobiology of aging* **42**, 150–162, https://doi.org/10.1016/j.neurobiolaging.2016.03.018 (2016).
23. van Dellen, E. *et al*. Loss of EEG Network Efficiency Is Related to Cognitive Impairment in Dementia With Lewy Bodies. *Movement disorders: official journal of the Movement Disorder Society* **30**, 1785–1793, https://doi.org/10.1002/mds.26309 (2015).
24. Bonanni, L. *et al*. EEG Markers of Dementia with Lewy Bodies: A Multicenter Cohort Study. *Journal of Alzheimer's disease: JAD* **54**, 1649–1657, https://doi.org/10.3233/jad-160435 (2016).
25. Olde Dubbelink, K. T. E. *et al*. Resting-state functional connectivity as a marker of disease progression in Parkinson's disease: A longitudinal MEG study. *NeuroImage: Clinical* **2**, 612–619, https://doi.org/10.1016/j.nicl.2013.04.003 (2013).
26. Bassett, D. S. *et al*. Hierarchical organization of human cortical networks in health and schizophrenia. *The Journal of neuroscience: the official journal of the Society for Neuroscience* **28**, 9239–9248, https://doi.org/10.1523/JNEUROSCI.1929-08.2008 (2008).
27. Olde Dubbelink, K. T. E. *et al*. Disrupted brain network topology in Parkinson's disease: a longitudinal magnetoencephalography study. *Brain: a journal of neurology* **137**, 197–207, https://doi.org/10.1093/brain/awt316 (2014).
28. Utianski, R. L. *et al*. Graph theory network function in Parkinson's disease assessed with electroencephalography. *Clinical neurophysiology: official journal of the International Federation of Clinical Neurophysiology* **127**, 2228–2236, https://doi.org/10.1016/j.clinph.2016.02.017 (2016).
29. O'Brien, J. T. *et al*. Diagnostic accuracy of 123I-FP-CIT SPECT in possible dementia with Lewy bodies. *The British journal of psychiatry: the journal of mental science* **194**, 34–39, https://doi.org/10.1192/bjp.bp.108.052050 (2009).
30. Garn, H., Coronel, C., Waser, M., Caravias, G. & Ransmayr, G. Differential diagnosis between patients with probable Alzheimer's disease, Parkinson's disease dementia, or dementia with Lewy bodies and frontotemporal dementia, behavioral variant, using quantitative electroencephalographic features. *J Neural Transm* **124**, 569–581, https://doi.org/10.1007/s00702-017-1699-6 (2017).
31. Snaedal, J. *et al*. Diagnostic Accuracy of Statistical Pattern Recognition of Electroencephalogram Registration in Evaluation of Cognitive Impairment and Dementia. *Dementia and geriatric cognitive disorders* **34**, 51–60 (2012).
32. Goldman, J. G., Williams-Gray, C., Barker, R. A., Duda, J. E. & Galvin, J. E. The spectrum of cognitive impairment in Lewy body diseases. *Movement Disorders* **29**, 608–621, https://doi.org/10.1002/mds.25866 (2014).
33. Emre, M. *et al*. Clinical diagnostic criteria for dementia associated with Parkinson's disease. *Movement disorders: official journal of the Movement Disorder Society* **22**, 1689–1707; quiz 1837, https://doi.org/10.1002/mds.21507 (2007).
34. Kurita, A., Murakami, M., Takagi, S., Matsushima, M. & Suzuki, M. Visual hallucinations and altered visual information processing in Parkinson disease and dementia with Lewy bodies. *Movement Disorders* **25**, 167–171, https://doi.org/10.1002/mds.22919 (2010).
35. Taylor, J. P. *et al*. Visual cortex in dementia with Lewy bodies: magnetic resonance imaging study. *The British journal of psychiatry: the journal of mental science* **200**, 491–498, https://doi.org/10.1192/bjp.bp.111.099432 (2012).
36. Taylor, J. P. *et al*. Visual hallucinations in dementia with Lewy bodies: transcranial magnetic stimulation study. *The British journal of psychiatry: the journal of mental science* **199**, 492–500, https://doi.org/10.1192/bjp.bp.110.090373 (2011).
37. Hanoglu, L. *et al*. Therapeutic Effects of Rivastigmine and Alfa-Lipoic Acid Combination in the Charles Bonnet Syndrome: Electroencephalography Correlates. *Current clinical pharmacology* **11**, 270–273 (2016).
38. Olbrich, H. M., Engelmeier, M. P., Pauleikhoff, D. & Waubke, T. Visual hallucinations in ophthalmology. *Graefe's Archive for Clinical and Experimental Ophthalmology* **225**, 217–220, https://doi.org/10.1007/bf02175452 (1987).

39. Frantzidis, C. A. *et al*. Functional disorganization of small-world brain networks in mild Alzheimer's Disease and amnestic Mild Cognitive Impairment: an EEG study using Relative Wavelet Entropy (RWE). *Frontiers in Aging Neuroscience* **6**, https://doi.org/10.3389/fnagi.2014.00224 (2014).
40. Reuter-Lorenz, P. A. & Cappell, K. A. Neurocognitive Aging and the Compensation Hypothesis. *Current Directions in Psychological Science* **17**, 177–182 (2008).
41. Lea-Carnall, C. A., Montemurro, M. A., Trujillo-Barreto, N. J., Parkes, L. M. & El-Deredy, W. Cortical Resonance Frequencies Emerge from Network Size and Connectivity. *PLoS computational biology* **12**, e1004740, https://doi.org/10.1371/journal.pcbi.1004740 (2016).
42. Łęski, S., Lindén, H., Tetzlaff, T., Pettersen, K. H. & Einevoll, G. T. Frequency Dependence of Signal Power and Spatial Reach of the Local Field Potential. *PLoS computational biology* **9**, e1003137, https://doi.org/10.1371/journal.pcbi.1003137 (2013).
43. Stoffers, D. *et al*. Slowing of oscillatory brain activity is a stable characteristic of Parkinson's disease without dementia. *Brain: a journal of neurology* **130**, 1847–1860, https://doi.org/10.1093/brain/awm034 (2007).
44. van der Hiele, K. *et al*. EEG and MRI correlates of mild cognitive impairment and Alzheimer's disease. *Neurobiology of aging* **28**, 1322–1329, https://doi.org/10.1016/j.neurobiolaging.2006.06.006 (2007).
45. Bosboom, J. L. W., Stoffers, D., Stam, C. J., Berendse, H. W. & Wolters, E. C. Cholinergic modulation of MEG resting-state oscillatory activity in Parkinson's disease related dementia. *Clinical Neurophysiology* **120**, 910–915, https://doi.org/10.1016/j.clinph.2009.03.004 (2009).
46. Fogelson, N. *et al*. Effects of rivastigmine on the quantitative EEG in demented Parkinsonian patients. *Acta neurologica Scandinavica* **107**, 252–255, https://doi.org/10.1034/j.1600-0404.2003.00081.x (2003).
47. Donaghy, P. C. & McKeith, I. G. The clinical characteristics of dementia with Lewy bodies and a consideration of prodromal diagnosis. *Alzheimer's Research & Therapy* **6**, 46 (2014).
48. McKhann, G. M. *et al*. The diagnosis ofdementia due to Alzheimer's disease: Recommendations from the National Institute on Aging-Alzheimer's Association workgroups on diagnostic guidelines for Alzheimer's disease. *Alzheimer's & dementia: the journal of the Alzheimer's Association* **7**, 263–269, https://doi.org/10.1016/j.jalz.2011.03.005 (2011).
49. Walker, M. P. *et al*. The Clinician Assessment of Fluctuation and the One Day Fluctuation Assessment Scale. Two methods to assess fluctuating confusion in dementia. *The British journal of psychiatry: the journal of mental science* **177**, 252–256 (2000).
50. Cummings, J. L. *et al*. The Neuropsychiatric Inventory: comprehensive assessment of psychopathology in dementia. *Neurology* **44**, 2308–2314 (1994).
51. Tomlinson, C. L. *et al*. Systematic review of levodopa dose equivalency reporting in Parkinson's disease. *Movement disorders* **25**, 2649–2653 (2010).
52. Oostenveld, R. & Praamstra, P. The five percent electrode system for high-resolution EEG and ERP measurements. *Clinical neurophysiology: official journal of the International Federation of Clinical Neurophysiology* **112**, 713–719 (2001).
53. Delorme, A. & Makeig, S. EEGLAB: an open source toolbox for analysis of single-trial EEG dynamics including independent component analysis. *Journal of neuroscience methods* **134**, 9–21, https://doi.org/10.1016/j.jneumeth.2003.10.009 (2004).
54. Hyv, A. Fast and robust fixed-point algorithms for independent component analysis. *IEEE Transactions on Neural Networks* **10**, 626–634 (1999).
55. Peraza, L. R., Asghar, A. U. R., Green, G. & Halliday, D. M. Volume conduction effects in brain network inference from electroencephalographic recordings using phase lag index. *Journal of neuroscience methods* **207**, 189–199, https://doi.org/10.1016/j.jneumeth.2012.04.007 (2012).
56. Stam, C. J., Nolte, G. & Daffertshofer, A. Phase lag index: assessment of functional connectivity from multi channel EEG and MEG with diminished bias from common sources. *Human brain mapping* **28**, 1178–1193, https://doi.org/10.1002/hbm.20346 (2007).
57. Whitham, E. M. *et al*. Scalp electrical recording during paralysis: Quantitative evidence that EEG frequencies above 20 Hz are contaminated by EMG. *Clinical Neurophysiology* **118**, 1877–1888, https://doi.org/10.1016/j.clinph.2007.04.027 (2007).
58. Hagemann, D. & Naumann, E. The effects of ocular artifacts on (lateralized) broadband power in the EEG. *Clinical Neurophysiology* **112**, 215–231, https://doi.org/10.1016/S1388-2457(00)00541-1 (2001).
59. Prim, R. C. Shortest Connection Networks And Some Generalizations. *Bell System Technical Journal* **36**, 1389–1401, https://doi.org/10.1002/j.1538-7305.1957.tb01515.x (1957).
60. Kaiser, M. A tutorial in connectome analysis: topological and spatial features of brain networks. *NeuroImage* **57**, 892–907, https://doi.org/10.1016/j.neuroimage.2011.05.025 (2011).
61. Freeman, L. C. Centrality in social networks conceptual clarification. *Social Networks* **1**, 215–239, https://doi.org/10.1016/0378-8733(78)90021-7 (1978).
62. Otte, W. M. *et al*. Aging alterations in whole-brain networks during adulthood mapped with the minimum spanning tree indices: the interplay of density, connectivity cost and life-time trajectory. *NeuroImage* **109**, 171–189, https://doi.org/10.1016/j.neuroimage.2015.01.011 (2015).
63. Rubinov, M. & Sporns, O. Complex network measures of brain connectivity: uses and interpretations. *NeuroImage* **52**, 1059–1069, https://doi.org/10.1016/j.neuroimage.2009.10.003 (2010).
64. Bounova, G. & de Weck, O. Overview of metrics and their correlation patterns for multiple-metric topology analysis on heterogeneous graph ensembles. *Physical Review E* **85**, 016117 (2012).

Acknowledgements

The research was funded by The Newcastle upon Tyne Hospitals NHS Charity, and supported by the Northumberland Tyne & Wear National Health Service (NHS) Foundation Trust and the National Institute of Health Research (NIHR) Biomedical Research Centre (BRC) at Newcastle University. S.G. was supported by the NIHR MedTech *In vitro* diagnostic Co-operatives scheme (ref MIC-2016–014). The study —participant recruitment and data collection— was funded by an intermediate clinical Wellcome Trust Fellowship (WT088441MA) to J.-P.T.

Author Contributions

L.R.P. executed the project, designed and performed the statistical analysis, and wrote the paper; R.C. and S.G. executed the project, and reviewed the paper; X.K. analysed data and reviewed the paper; M.J.F. contributed on the design of the experiments and reviewed the paper; A.K. executed the study and reviewed the paper; A.J.T. and J.T.O.'B. performed research; J.-P.T. Designed the study, performed research and reviewed the paper.

Additional Information

Supplementary information accompanies this paper at https://doi.org/10.1038/s41598-018-22984-5.

Competing Interests: The authors declare no competing interests.